

A MODEL STUDY OF A FOLDED PLATE STRUCTURE

by

SHIH YING CHANG

Diploma, Taipei Institute of Technology, Taiwan, China

A MASTER'S THESIS

submitted in partial fulfillment of the

requirements for the degree

MASTER OF SCIENCE

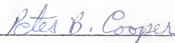
Department of Civil Engineering

Kansas State University

Manhattan, Kansas

1969

Approved by:


Major Professor

2668
74
1969
142

TABLE OF CONTENTS

	Page
ABSTRACT	
I. INTRODUCTION	1
II. LITERATURE SURVEY.	3
A. Review of Literature on Methods of Analysis.	3
1. Beam Method.	3
2. Winter and Pei's Method.	4
3. Gesund's Method.	5
4. Slope Deflection Method.	6
5. ASCE Recommended Method.	8
6. Minimum Energy Method.	9
B. Review of Model Studies of Folded Plate Structures	10
1. Edward A. Zononi, "Model Studies of a Folded Plate Structure"	10
2. Pierre Chevin, "Study of a Folded Plate Structure"	10
3. Scordelis, A. C. and Gerasimenko, P. V., "Strength of Reinforced Concrete Folded Plate Model	10
4. Chacos, G. P. and Scalzi, J. B., "Ultimate Strength of A Folded Plate Structure".	11
III. EXPERIMENTAL PROGRAM	
A. Description of Model and Test Setup.	12
B. Determination of Material Properties	14
1. Tests of the creep characteristics of the material	14
2. Tests to determine the Modulus of Elasticity and Poisson's ratio.	15
C. Test of Folded Plate Model	16
IV. COMPARISON OF TEST RESULTS WITH THEORETICAL PREDICTIONS.	20
V. CONCLUSIONS.	24
VI. SUGGESTIONS FOR FUTURE RESEARCH.	25
ACKNOWLEDGEMENTS	26
REFERENCES	27
TABLES AND FIGURES	29

I. INTRODUCTION

A prismatic folded plate structure is a shell consisting of a series of flat plates, mutually supporting each other along their longitudinal edges, that frame into transverse end diaphragms. Folded plates have been used extensively in the construction of long-span roof systems because of their economy and their interesting architectural appearance. Many other applications of this type of structure are possible in buildings, bridges, airplanes, and missiles.

The first folded plate structures were constructed in Germany during the 1920's for use as coal bunkers and similar structures where the ratio of span-to-width of plate is relatively small¹. Technical papers on this subject began appearing about 1930. The first application in the United States may have been a warehouse in San Francisco designed by L. H. Nishkian, Consulting Engineer, and built about 1935¹.

In recent years, folded plates have been used for a large variety of structures and are of increasing importance in the building industry as the basis of a new system of construction.

Numerous theories on the analysis of folded plates can be found in engineering literature. For example, the beam method^{2,3,4}, Winter and Pei's method^{5,6}, Gesund's method^{6,7}, the slope deflection method^{8,9}, the ASCE Recommended method^{10,11}, and the minimum energy method¹², have all been used to analyze folded plates.

These different theories have some common assumptions, but because the theories are different, the results vary from one method to another. The purpose of the investigation described in this thesis was to test a

model of a folded plate structure and to compare the experimental results with results obtained from the theories listed above. From this comparison, an indication was obtained as to which theories are more reasonable for actual folded plate structures.

The investigation was limited in scope to experiments on one plexiglas model of a folded plate structure, and a comparison of the experimental results with the above six different methods of analysis.

II. LITERATURE SURVEY

A. Review of Literature on Methods of Analysis

Numerous technical papers have been written on methods of analyzing folded plate structures. The design method most commonly used in the United States was introduced by Winter and Pei⁵, and was later modified by Gaafar⁶ by introducing the effect of joint displacements. Subsequent treatments of this approach have been made by many others. These methods are based on several simplifying assumptions regarding structural behavior. These will be described in detail in this section.

1. Beam Method^{2,3,4}

In some cases, designers have used the elementary beam theory of strength of materials to calculate stresses in folded plate structures. In general, an analysis by this method will yield stresses considerably different from the actual stresses in the structure.

The general flexure formula can be used to determine longitudinal stresses provided that the following assumptions are fulfilled:

- a. The material is elastic, isotropic, and homogeneous.
- b. The structure is completely monolithic.
- c. The longitudinal fiber strains and stresses have a planar distribution over the entire cross section.
- d. As a result of assumptions c, all points on a given cross section experience the same resultant deflection; therefore, there is no transverse distortion of the cross section.
- e. The resultant of the external loads passes through the shear center of the cross section.

- f. Supporting end diaphragms are infinitely stiff parallel to their own plane.

For the loading on the plexiglas model in this investigation assumption e. is satisfied for symmetrical loading only, because the shear center is located at the centroid of the cross-section, and for symmetrical loading the external loads are applied through this centroid. Thus, according to the beam theory, there is no tendency for twist.

Condition d, and thus, condition c are generally not satisfied in a folded plate structure, because the thin plates forming the cross section do not provide a sufficiently stiff transverse slab system to make the transverse distortion of the cross section negligible.

2. Winter and Pei's Method^{5,6}

The following basic assumptions are made in all methods considered for this study except the beam method.

- a. The material is homogeneous, isotropic, and linearly elastic.
- b. The actual deflections are minor relative to the overall configuration of the structure. Consequently, equilibrium conditions for the loaded structure may be developed using the configuration of the undeflected structure.
- c. The principle of superposition holds; this assumption is derivable from the previous two assumptions.
- d. Longitudinal joints are fully monolithic with the slab acting continuously through the joints.
- e. Each supporting end diaphragm is infinitely stiff parallel to its plane but is perfectly flexible normal to its plane.

Winter and Pei provided a convenient solution neglecting the effect of the relative displacements of the joint. In this analysis, the roof in the transverse direction is considered as a continuous one-way slab supported on rigid supports at the joints and thus the shear forces R are readily obtained. The R -forces at each joint are then resolved into two component P -forces parallel to the contiguous plates. The plates, acting as beams between the diaphragms, carry the P -loads (plate action). At the same time, edge shear stresses (V) are created along the edges to maintain equal longitudinal strains along the common edge. The longitudinal plate stresses at a section of the roof, caused by the P -forces only, are corrected by those longitudinal edge forces.

It is concluded that the longitudinal edge forces, in addition to the bending moment M caused by the normal loads P , can be calculated in the same way as the three moment equation for continuous beams.

3. Gesund's Method^{6,7}

There are several methods based on the same theory as Gesund's method,^{6,7} for example Yitzhaki's method⁹, Vlassow's method¹⁴, Portland Cement Association Bulletin¹⁵, and the Iteration method¹⁶. In the present study, the author used Gesund's procedure to calculate the stress at each ridge.

The analysis used in this procedure may be summarized in two parts: The first step is the elementary analysis which is based on Winter and Pei's approach. The procedures and the equations are different, but the results are identical. Fig. 1 shows the sign and loading convention of this method.

The second step is a correction analysis; this step is to calculate edge deflections and to correct the moments and stresses previously obtained by either of two different procedures:

- (1) After obtaining the first correction edge moments m^I , plate moments M^I , and edge forces N^I to the original m , M , N , which are due to elementary analysis, by either solving simultaneous equations or using the pseudo moment-distribution method, a new deformation of the plate Δ^I will be caused, which in turn leads to m^{II} , M^{II} , N^{II} . The calculation process may be repeated as often as is necessary to reduce the corrections to small values. Finally, all the corrections may be added together and then added to the first values of m , M , and N for the final results. If this method of successive corrections diverges, it probably means that the proportions of the structure are such as to make it too flexible.
- (2) Another way of correcting for the motion of the edges is similar to the method of sidesway correction for moment distribution in multistory frame. It was first reported by Gaafar⁶.

4. Slope Deflection Method^{8,9}

The structure may be thought of as a continuous one-way slab, that is, supported by the joints of the plate structure, the plate structure being loaded at the joints by the reactions of one-way slabs.

In the main system, the joints are assumed to be hinged and the moments m are applied along the joints to secure the continuity of the slab in the transverse direction. The unknown moments are determined.

from the slope-deflection equations. The main system is subjected first to external load only, while the moments at the joints are assumed to be zero (this first step is based on Winter and Pei's method), and second to the loading of unit joint moment m acting separately. The continuity of the slab at a joint is maintained if the slope-deflections of adjacent slabs, produced by the external load and by all the joint moment loads acting simultaneously, reduce to zero.

In a folded plate, the slope-deflections vary longitudinally along the joints. The slope-deflections can be made to vary similarly along the structure; that is, the corresponding slope deflection at every transverse strip will be proportional to the maximum ordinate. In that case, securing of continuity across any slab strip assures the continuity across every strip, that is, along the entire structure. The continuity equations of a slab strip are the same as those of a continuous beam.

The slope-deflection equations are established for the transverse strip of slab at the distance X , at which the θ -values are maximum and $f(x) = 1$. Let only three unknown moments m_2 , m_3 , and m_4 occur at the respective joints 2, 3, 4 of the structure. The terms θ_{20} , θ_{30} , θ_{40} denote the slope-deflections at the joints 2, 3, 4 caused by the action of the external loads only, while the moments at the joints are zero ($m_2 = m_3 = m_4 = 0$); θ_{22} , θ_{32} , θ_{42} , denote the slope-deflections at the respective joints caused by the unit moment m_2 acting along joint 2 [loading $m_2 = 1 f(x)$], with the same meaning of θ_{23} , θ_{33} , θ_{43} , and θ_{24} , θ_{34} , θ_{44} . Then the slope-deflections are

$$\theta_2 = \theta_{20} + \theta_{22}m_2 + \theta_{23}m_3 + \theta_{24}m_4 = 0$$

$$\theta_3 = \theta_{30} + \theta_{32}m_2 + \theta_{33}m_3 + \theta_{34}m_4 = 0$$

$$\theta_4 = \theta_{40} + \theta_{42}m_2 + \theta_{43}m_3 + \theta_{44}m_4 = 0,$$

These equations are solved for the m -values.

The final stresses σ_n are calculated by superposition. The value σ_n at n consists of σ_{n0} due to external loading and the σ produced by the joint moments, assuming the case of three unknown moments m_2, m_3, m_4 .

5. ASCE Recommended Method^{10,11}

This analysis method is divided into three parts: The first part, an elementary analysis, consists of two steps: (a) Transverse slab analysis - all surface loads are considered as carried transversely by the plates acting as continuous one-way slabs spanning between the unyielding supports at the folds or joints; (b) Longitudinal plate analysis - all loads carried transversely to the joints are considered as transferred longitudinally to the end supporting members by the plates acting as inclined simple beams. Plate deflections computed from the longitudinal plate analysis will show that some relative displacement occurs between successive joints, thus violating the basic assumption of the transverse slab analysis, i.e., unyielding supports.

The second part is a correction analysis. In order to correct for the relative joint displacements created in the elementary analysis, the general procedure is to apply an arbitrary relative joint displacement successively to each plate and compute the resulting plate deflections S . These plate deflections are then related by geometry to the arbitrary relative joint displacements and a number of simultaneous

equations equal to the number of restrained plates are written and solved for the actual relative joint displacements.

The third part uses superposition, in which the results of the elementary analysis are combined with those of the correction analysis to give the final values.

6. Minimum Energy Method¹²

The minimum energy principle states that the actual configuration of an elastic structure deformed by loading is such that the total potential energy, which consists of the potential energy of the applied load and the strain energy of the deformed structure, is a minimum. Based on this principle, folded plate problems can be solved. The expressions for the deflections of the structure are selected such that (a) the boundary conditions of deflection are fulfilled, (b) the shape of the deflection curve is generally in accord with the expected deflected shape, and (c) the actual shape and amplitude of the curve is defined by a set of undetermined coefficients. The total potential is then expressed in terms of these undetermined coefficients. The fact that the total potential is a minimum with respect to each such coefficient is utilized by setting the derivative of total potential with respect to each coefficient equal to zero. Thus, as many independent linear equations involving the coefficients are obtained as there are coefficients and the coefficients are then evaluated. Once the deflection curves are determined, the various stress resultants are readily obtainable.

B. Review of Model Studies of Folded Plate Structures.

1. Edward A. Zanoni, "Model studies of a Folded Plate Structure"¹⁷

A model was fabricated consisting of five plexiglas plates (Fig. 2). Each plate had a width of 5" and a thickness of 1/8". The model was 18" long. It was tested under various loadings, and the test results were compared with theoretical values. Two main conclusions were made:

- a. "The correction of longitudinal stresses in the folded plate structure due to differential joint displacements is extremely important."
- b. "When proper techniques are employed, plexiglas model studies can be performed very simply. Results that are comparable to theoretical predictions have been obtained in these studies."

2. Pierre Chevin, "Study of A Folded Plate Structure"¹⁸

The author followed the procedure of Zanoni¹⁷, testing the same model for various loading conditions including symmetrical ridge line loads and unsymmetrical ridge line loads. For each of these cases a theoretical solution was compared with the test results in order to check the validity of the theory. Based on the method of Yitshaki⁹, the author also tested three kinds of structural supports, middle columns and a tie placed at the top of the vertical walls. The experimental results showed good agreement with the theoretical analysis.

3. Scordelis, A. C. and Gerasimenko, P. V., "Strength of Reinforced Concrete Folded Plate Model"¹⁹.

Two similar reinforced concrete models were designed, model A based on the elasticity method and model B based on elementary beam theory.

Both models had the same over-all plan dimensions (30" by 20") and used 14 - gage (0.08 - in. diameter) annealed "tie wire" as steel reinforcement (Fig. 3). The models were loaded at each interior joint with eight equal concentrated loads to approximate a distributed line load. It was concluded that the models exhibited similar behavior. Ultimate failure occurred at four and one-half times the full design load in both cases and was caused by diagonal tension cracking near the supports and cracking in the supporting diaphragms, which was produced by warping of the diaphragms due to the longitudinal strains in the folded plate elements. It was also concluded that folded plate theory can be used to predict the behavior in the working load range.

4. Chacos, G. P. and Sealzi, J. B., "Ultimate strength of a Folded Plate Structure"²⁰

A model was tested to determine the behavior of folded plate structures under different loading. This folded plate model had an irregular cross section and was tested as a simple beam to verify the ultimate moment capacity by the rectangular stress - block method. The ultimate collapse load of the model agreed with the theoretical load within 1.8 percent.

III. EXPERIMENTAL PROGRAM

A. Description of Model and Test Setup

Fig. 4 shows the dimensions and cross-section of the folded-plate model, which was based on the structure discussed in a recent report by the Task Committee on Folded-plate Construction¹⁰. The scale factor was 1/32. The model consisted of six plates: plate 1 and 6 with a thickness of 3/16" (0.1875") and plates 2, 3, 4, and 5 with a thickness of 1/8" (0.125"). Plates 2 and 5 form an angle of 30° with the horizontal while plates 3 and 4 are 10° from the horizontal. The two end diaphragms were made of the same thickness material as plates 1 and 5, and the entire system of plates were fastened together at their joints with a solvent cement.

The model material was plexiglas II U.V.A., clear plates. Many model tests have been performed on aluminum models^{6,21}, with very gratifying results. However, plexiglas has also been used recently with very good results. The advantage of plexiglas over aluminum is that the strains will be considerably higher for the same stress condition, permitting the use of much smaller loads with a plexiglas model. Some of the disadvantages of working with plexiglas are the variation of the Modulus of Elasticity from sheet to sheet and the difficulty in obtaining reliable strain gage data from plexiglas specimens.

The problem of the variation of Modulus of Elasticity can best be coped with by conducting tensile coupon tests on coupons cut from each plate. A technique for obtaining reliable strain gage readings on the plexiglas model is discussed later.

As for the test setup, there were only four points of contact for the

reactions. Two small indentations was made in each end diaphragm so that small steel balls could be used as point supports as shown in Fig. 4. With these supports the ends of the model could rotate freely. A model as light in weight as this one must be carefully loaded so that it will not move laterally, or come off the point supports.

As shown in Fig. 5, the folded plate model was instrumented with 16 SR-4 electrical resistance strain gages to record longitudinal strains at selected points on the plates. These were arranged in pairs with one gage on the top face of the plate and another gage at the same point on the bottom face, that is two gages at the same point on the different faces to measure the longitudinal strains.

Fig. 6 shows the location of the strain gages. Gages 1, 2, 3, 4, 5, 6, 7, and 8 were placed on the top of the model, while gages 1', 2', 3', 4', 5', 6', 7', and 8' were placed on the bottom face of the model. Gages 1, 2, 3, 4, 1', 2', 3', and 4', were placed at midspan and gages 5, 6, 7, 8, 5', 6', 7', and 8' were placed 2" from the end diaphragm.

The model was loaded at each interior joint by eight equal concentrated loads to approximate a distributed line load. Loads were applied through a "Loading Tree" system as shown in Fig. 7. To transmit the loads to the structure, nylon threads were tied to the load points on the model.

The "Loading Tree" served to divide the applied load into eight equal parts to simulate a line loading. To load the model, therefore, one concentrated load was applied at one end of the loading tree system, and the load was transmitted to the structure in terms of line loading over the length of the model. For static loading of models such as this, this system is extremely practical and the loading can be controlled quite

accurately.

The dead weight of the loading system and the model itself existed prior to taking the zero readings.

B. Determination of Material Properties.

Prior to testing the folded plate model, some preliminary tests were made to determine various characteristics of the plexiglas and also to verify the behaviour of the strain gages. The physical properties obtained from these tests included the Modulus of Elasticity, the creep characteristics and Poisson's ratio.

The general dimensions of the tensile coupons are shown in Fig. 8. One coupon was 1/8" thick, and the other was 3/16" thick. Two SR-4, A-75 strain gages were mounted on each tensile coupon, one to measure longitudinal strain, and the other to measure transverse strain. In order to test under constant loading, a small hole was drilled at each end of each coupon on the center line. After tying a nylon loop at each hole, constant loads were applied using weights.

1. Tests of the creep characteristics of the material.

The first series of tests were intended to investigate the creep characteristics of the material. Since this involves a time factor, a constant load was applied and readings taken in 10-second intervals up to 1 minute, and thereafter in one minute intervals until the strain readings were sufficiently stable. The total testing time for these tests was 10 minutes.

The coupon tests were conducted at different load levels. For the 1/8" x 1/2" cross-section a stress level of 320 psi was used, that is, the applied load was 20 lbs. The relationship between strain and time

for this test is shown in Fig. 9, from which it can be seen that after five minutes the strain reading were sufficiently stable.

Similarly, the coupon with a 3/16" x 1/2" cross section was loaded with 30 lbs, resulting in the same stress level (320 psi). Similar results were obtained from this test.

From the two creep tests, it is obvious that strain is a function of time, and that strain readings after five minutes of loading were sufficiently stable. This means that the tensile coupons had negligible creep effects after applying a constant load for five minutes.

2. Tests to determine the Modulus of Elasticity and Poisson's ratio.

From the creep tests it was known that the tensile coupons had negligible creep effects after five minutes of loading. The following tests were based on this experience, in that strain readings were taken exactly five minutes after a load had been applied.

When electrical resistance strain gages are used on plexiglas, the heat generated in the gage due to current passing through it can affect the behavior of the plexiglas in the immediate vicinity of the gage. To overcome this problem, a procedure was developed whereby current was applied to each gage for exactly 20 seconds before reading the strain. This period was sufficient to permit the strain indicator to stabilize. Since the difference between the strain at zero load and that at some applied load was the data needed from each test, the use of the same 20 second gage warmup period for all readings resulted in the elimination of the local heating effect when strain differences were calculated. The effectiveness of this procedure was established when identical strain differences were obtained when a load test was repeated.

Using the procedures described above, load was applied in increments of 5 lb. up to 30 lb. for the coupon having the 1/8" x 1/2" cross section, and in increments of 5 lb up to 25 lb for the coupon with the 3/16" x 1/2" cross section. After each loading increment the applied load was removed, and the coupon was allowed to recover. The procedure was then repeated with succeeding load increments.

For the first coupon test, Fig. 10 shows the relationship between load and strain, while in Fig. 11 the relationship between transverse strain and longitudinal strain is presented. The slope of the curve of Fig. 10 divided by the cross section of the coupon is the Modulus of Elasticity. From this test a value of $E = 479^{\text{ksi}}$ was obtained. The slope of the curve of Fig. 11 is Poisson's ratio ($\mu = 0.36$).

From the test on the coupon with the 3/16" x 1/2" cross section the Modulus of Elasticity was 476^{ksi} and Poisson's ratio was 0.39.

The values of Modulus of Elasticity and Poisson's ratio used in all subsequent calculations for the folded plate model were based on the average of the values obtained from the two coupon tests.

From the tensile coupon tests, it was concluded that:

- a. The strain readings would become sufficiently stable after five minutes of constant loading.
- b. A constant gage warmup period of 20 seconds could be used, thereby eliminating the local heating effect.
- c. The Modulus of Elasticity for the plexiglas is 477.5^{ksi}
- d. Poisson's ratio is 0.375.

C. Test of Folded Plate Model.

With regard to the creep problem, the procedure for testing the folded plate model was the same as that used for the tensile coupon

tests, that is, a time interval of five minutes was permitted to elapse between application of a load increment and reading the strain gages. Also, the same 20 second gage warmup period was used to eliminate the local heating effect, so about 10 minutes was required for each load increment including reading the 16 strain gages.

The loading was accomplished by means of the "Loading Tree" system previously described (Fig. 7), and applied loads of 10 lb., 20 lb., 30 lb., and 50 lb. were included in each loading case. The dead weight of the Loading Tree system and the model itself existed prior to the readings taken to be at zero load. In order to check the recovery of the model, each time a load increment was applied and strain reading recorded the load was returned to zero.

The test results are divided into three parts according to the loading locations (Fig. 12); line loading at Line 2, line loading at Line 3, and line loading at Line 4.

The results of the test with line loading at Line 2 are presented in Figs. 13 and 14, which consists of eight plots of applied load versus measured strain corresponding to the eight gage locations on the model (Fig. 6). The measured strain values plotted in Figs. 13 and 14 are the averages of the reading of the two gages at each point. For example; at gage point 1, the measured strains from gage 1 and 1' were 30×10^{-6} in/in, and 60×10^{-6} in/in, respectively, due to an applied load of 10 lbs. The average of these values (45×10^{-6} in/in) is plotted as point A in Fig. 13. By taking the average of the two gage readings at each gage point, plate bending strains are eliminated and the average longitudinal, in-plane strains are obtained for later

comparison with values computed based on the various folded plate theories.

Similar results for line loading at Lines 3 and 4 are shown in Fig. 15 to 18, respectively. For each gage point and loading position, a straight line has been drawn through the plotted points. It is evident from Fig. 13 to 18 that the model behavior was linear and elastic. The data also indicates that the creep and local heating problems previously discussed were successfully overcome.

From the linear load-strain relationships of Figs. 13 to 18 values of the "unit strain" for each gage point and line loading can be determined. "Unit strain" is defined as the strain caused by a unit line load and is the inverse of the slope of a load-strain curve. For example; at gage point 1, for loading at Line 2 (see Fig. 13), the inverse of the slope is plus 5.38×10^{-6} in/in/lb. Similar results for other gage points and for loading at Lines 3 and 4 are shown in Figs. 13 to 18.

The unit strain values obtained from the symmetrical loading case (loading on Line 3) can be checked by the use of symmetry as shown in Table 1. For example, the unit strain at gage point 1 should be the same as that for gage point 4. The average of these two unit strain values is given in column 4 at Table 1, while the percent deviation is listed in column 5, (0.8%). Similar results are presented in the table for the other gage points, with a maximum value of the percent deviation equal to 8.1%. Using the average unit strain values and the value of E determined from the coupon tests, the stress due to a line load of 50 lb. has been calculated and listed in the last column

of Table 1 for later comparison with theoretical calculations.

The unit strain values for unsymmetrical loadings (loading on Lines 2 and 4) can be checked against one another by the use of Maxwell's Law, which can be stated: the unit strain at point m due to a line loading at point n is equal to the unit strain at point n due to a line loading at point m. The check on the unit strain values for unsymmetrical loading is presented in Table 2 in a manner similar to Table 1. The maximum deviations from the average unit strain is 9.0%. Stresses due to a line load of 50 lb. are listed in the last column of Table 2 for later comparison with analytical results.

The percent deviations in Table 1 and 2 definitely show that the model gave consistent results. These values are also an indication that the test set up was stable and that the model recovered from the various loading conditions extremely well.

IX. COMPARISON OF TEST RESULTS WITH THEORETICAL PREDICTION

The longitudinal plate bending stresses in a plate which is a component of a folded plate structure are shown in Fig. 19a. At ridges $n-1$ and n the corresponding longitudinal stresses are σ_{n-1} and σ_n respectively. From the theoretical calculations using the various methods, the longitudinal bending stresses were calculated for each ridge (σ_{n-1} and σ_n for plate n). The stress distribution in a plate between the two ridges is linear, therefore, if the ridge stresses are known the stresses at any point in the plate between ridges can be calculated very simply. In the folded plate model tests of this investigation the strain gages were located at points between the ridges (Fig. 6). There were two strain gages at each point, one on the top face of the plate, the other on the bottom face. The experimental value of the stress at the center of the plate at a gage point was calculated as follows: if σ_1 is the stress measured by the gage on the top face of the plate and σ_2 is the stress measured by the gage on the bottom face of the plate, then the stress at the center of the plate is the average of these two stresses $(\frac{\sigma_1 + \sigma_2}{2})$, as shown in Fig. 19b.

Fig. 19b also shows the technique used to compare theoretical and experimental values of the longitudinal stresses. The stresses σ_a and σ_b represent the values calculated by theoretical methods at the gage points, while the stresses σ'_a and σ'_b represent the values determined from the strain gage measurements. Then $\sigma_a - \sigma'_a$ and $\sigma_b - \sigma'_b$ are the differences between the theoretical and experimental values.

The longitudinal stresses at each ridge of the model as determined by the various theoretical methods are listed in Tables 3 and 4. The

theoretical stresses are compared with measured values for each gage point in Tables 5 and 6. In these tables are listed in differences between the theoretical and experimental stresses for each analysis method as well as the percent difference between the two values. A discussion of the various analysis methods and their comparison with the experimental results follows.

A. Beam method.

According to the assumptions of the beam method, twist is not permitted in the structure, that is, the resultant of the external loads should pass through the shear center of the structure. In order to satisfy this assumption, only the experimental results for a symmetrical load on the structure (line load at Line 3), can be compared with the predictions based on the beam theory. Fig. 20 shows this comparison, with solid lines representing the stresses according to beam theory and the circled points representing the test results. The theoretical predictions are very bad for both the gage points near the center of the structure where the load is applied and near the ends. As Table 5 shows, the percent difference between the predicted and experimental stresses ranges from + 67.0% (gages 2 and 3) to - 77.4% (gages 1 and 4) at midspan, and from -60.0% (gages 6 and 7) to - 68.6% (gages 5 and 8) at the section 2" from the end.

This result is obtained because the structure does not behave as a unit according to the ordinary beam theory, that is, the longitudinal stresses are not proportional to the distance from the centroid of the entire cross section as they would be in the case of beam action. The beam method may not even predict the correct sense of the longitudinal

stresses.

B. Winter and Pei's Method:

Winter and Pei's method can be used for both symmetrical and unsymmetrical loads. In the case of symmetrical loads (Fig. 21) the theoretical predictions have the correct sense near the loaded ridge at the center of the structure, but at the other gage points, near the edges, they have opposite signs from the experimental results. Table 5 shows that the percent difference between the stresses varies from + 184.1% (gages 2 and 3) to - 172.2% (gages 1 and 4) at midspan, and from + 235.0% (gages 6 and 7) to - 201.1% (gages 5 and 8) 2" from the end. In the case of unsymmetrical loads (Fig. 22) Winter and Pei's method does not result in as good correlation either, with stresses of opposite signs being obtained at several points. As Table 6 shows, the percent differences are + 543.0% (gage 1) and - 432.1% (gage 2) at the midspan, and + 1090% (gage 7) and - 204.0% (gage 6) 2" from the end.

The lack of agreement between the predictions based on Winter and Pei's method and the test results can be attributed to the fact that, in this method of analysis, the effect of relative joint displacements are neglected.

C. Methods Considering Effect of Joint Displacements

When relative joint displacements are considered in the theoretical calculations, for example, calculation based on Gesund's method (Figs. 23 and 24), the slope deflection method (Figs. 25 and 26), the ASCE recommended method (Figs. 27 and 28), and the energy method (Figs. 29 and 30), much better agreement between experimental and theoretical values is obtained than is the case using methods which neglect relative joint

displacements. It is obvious from the figures that under both symmetrical and unsymmetrical loadings, these methods predict the correct sense in every case and provide a fairly reasonable estimate of the stress values. Because this plexiglas model is very flexible, the percent differences between the theoretical and experimental stresses shown in Table 5 and 6 are somewhat misleading in some cases where the predicted stresses are small and small differences in stress magnitudes result in large values of percent differences.

All of the four analytical methods which account for relative joint displacements provided a fairly good estimate of the experimental results for both symmetrical and unsymmetrical loads. It is obvious that these results emphasize the importance of including the effects of relative joint displacements in the analysis of folded plate structures.

V. CONCLUSIONS

On the basis of the study reported herein, the following conclusions may be advanced regarding the behavior of plexiglas folded plate models and the methods of analysis for folded plate structures:

1. Plexiglas can be used as a model material with reasonable results. The advantage of plexiglas over metals is evident in that the strains will be considerably higher for plexiglas than for metals under the same stress condition, permitting the use of much smaller loads on the plexiglas.
2. When proper precautions are taken, the creep and strain gage warm-up problems can be overcome in testing plexiglas models, resulting in consistent and reproducible data.
3. The stresses calculated by approximate methods (the beam method and Winter and Pei's method) which neglect relative joint displacements, are significantly in error with experimental results with regard to both magnitude and distribution across the cross section.
4. The Gesund's method, the slope deflection method, the ASCE recommended method, and the energy method are alternate methods to each other; although the analytic procedures and equations differ, the results are practically equivalent.
5. The stresses calculated by the methods which consider relative joint displacements, for example, the Gesund's method, the slope deflection method, the ASCE recommended method, and the energy method, agree fairly well with experimental results.

VI. SUGGESTIONS FOR FUTURE RESEARCH

The following are recommended as subjects for future research:

1. Additional research is needed to compare the theoretical results with experimental results using different type of folded plate structures and different end conditions.
2. Because most folded plate structures are made of reinforced concrete, research should also be conducted to investigate the behavior of reinforced concrete folded plate models, first in the design load range, after which ultimate load tests could be conducted to check the various ultimate strength theories.
3. A lateral load study, and a torsion study could be performed in future research.
4. The edge beams of the folded plate could be subjected to prestress, with the prestressing forces treated as external loads and the stresses produced by them superimposed on those caused by the loads on the structure.

ACKNOWLEDGEMENTS

The model studies for this thesis were conducted in the Structural Models Laboratory of the Dept. of Civil Engineering at Kansas State University.

The author wishes to express his sincere appreciation and gratitude to his advisor, Dr. Peter B. Cooper, for devoting a great deal of his time to instructing and guiding the author during the investigation.

Appreciation is also expressed to Dr. Jack B. Blackburn, Head of the Department of Civil Engineering; Professor Vernon H. Rosebraugh, and Dr. Chen-Jung Hsu for serving on the advisory committee and for reviewing the manuscript.

Thanks are due to Mr. Wallace Johnson for his careful fabrication of the model and for his helpful suggestions on model design and testing techniques.

REFERENCES

1. Whitney, Charles S., "Reinforced Concrete Folded Plate Construction," Journal of the Structural Division, ASCE, Vol. 85, No. ST8, October 1953.
2. Scordelis, A. C., Croy, E. L. and Stubbs, I. R., "Experimental and Analytical Study of a Folded Plate," Journal of the Structural Division, ASCE, Vol. 87, No. ST8, December 1961.
3. Borg, Sidney F., Advanced Structural Analysis, McGraw-Hill Book Co., 1958.
4. Chinn, J., "Cylindrical Shell Analysis by Beam Method," Proceedings, ACI, Vol. 55, May 1959.
5. Winter, G. and Pei, M., "Hipped Plate Construction," Journal, ACI, Vol. 43, No. 5, January 1947.
6. Gaafar, I., "Hipped Plate Analysis Considering Joint Displacement," Transactions, ASCE, Vol. 119, 1954.
7. Dunham, Clarence W., Advanced Reinforced Concrete, McGraw-Hill Book Co., 1964.
8. Yitshaki, D., and Reiss, Max, "Analysis of Folded Plates," Journal of the Structural Division, ASCE, Vol. 88, No. ST5, October 1962.
9. Yitshaki, D., Prismatic and Cylindrical Shell Roofs, Haifa Science Publishers, Haifa, Israel, 1958.
10. "Phase I Report on Folded Plate Construction," Report of the Task Committee on Folded Plate Construction, Journal of the Structural Division, ASCE, Vol. 89, No. ST6, December 1963.
11. Billington, David P., Thin Shell Concrete Structures, McGraw-Hill Book Co., 1965.
12. Fialkow, M. N., "Folded Plate Analysis by Minimum Energy Principle," Journal of the Structural Division, ASCE, Vol. 88, No. ST3, June 1962.

13. Kinney, J. S., Indeterminate Structure Analysis, Addison Wesley Publishing Co., Inc., 1967.
14. Traun, Eliaha, "Design of Folded Plates," Journal of the Structural Division, ASCE, Vol. 85, No. ST8, October 1959.
15. "Direct Solution of Folded Plate Concrete Roofs," Advanced Engineering Bulletin No. 3, Portland Cement Association, 1960.
16. Brielmaier, A. A., "Prismatic Folded Plates," Proceedings, ACI, Vol. 59, March 1962.
17. Zanoní, E. A., "Model Studies of a Folded Plate Structure," M. S. Thesis, Lehigh University, Bethlehem, Pennsylvania, 1962.
18. Chevin, Pierre, "Study of a Folded Plate Structure," M. S. Thesis, Lehigh University, Bethlehem, Pennsylvania, 1963.
19. Scordelis, A. C. and Gerasimenko, P. V., "Strength of Reinforced Concrete Folded Plate Models," Journal of the Structural Division, ASCE, Vol. 92, No. ST1, February 1966.
20. Chacos, G. P. and Scalzi, J. B., "Ultimate Strength of a Folded Plate Structure," Proceedings, ACI, Vol. 57, February 1961.
21. Scordelis, A. C., "Experimental and Analytical Study of a Folded Plate," Journal of the Structural Division, ASCE, Vol. 87, No. ST8, December 1961.

Section location	Gage point	Unit strain (10^{-6}) in/in $\frac{-1b}{-1b}$	Ave. unit strain (10^{-6}) in/in $\frac{-1b}{-1b}$	% Deviation from ave. strain	Stress due to P=501b, psi (E=477.5ksi)
Mid span	1	+10.2	+10.1	0.8	+241
	4	+10.0			
	2	-10.5	-10.3	1.4	-245.0
	3	-10.2			
2 inches from end	5	+2.0	+2.0	2.8	+48.9
	8	+2.1			
	6	-2.6	-2.4	8.1	-58.4
	7	-2.2			

Table 1 Check on Unit Strain Values and Stress Calculation
(Symmetrical Loading)

Section Location	Gage Point	Unit Strain $\frac{-6}{(10)} \frac{\text{in/in}}{\text{lb}}$	Ave. Unit Strain $(10^{-6}) \frac{\text{in/in}}{\text{lb}}$	% Depletion from Ave. Strain	Stress due to P=50 lb (E=477,50 ksi)
	Gage 1, Line 2	+5.38	+5.27	2.1	+125.1
	Gage 4, Line 4	+5.17			
	Gage 2, Line 2	-4.9	-4.71	3.3	-112.1
	Gage 3, Line 4	-4.53			
Mid Span	Gage 3, Line 2	-0.7	-0.69	1.4	-16.4
	Gage 2, Line 4	-0.68			
	Gage 4, Line 2	+1.2	+1.28	6.3	+30.4
	Gage 1, Line 4	+1.3			
	Gage 5, Line 2	+2.5	+2.58	3.1	+61.2
	Gage 8, Line 4	+2.65			
	Gage 6, Line 2	-1.19	-1.17	1.7	-27.8
	Gage 7, Line 4	-1.15			
2 inches from end	Gage 7, Line 2	+0.5	+0.45	9.0	+10.7
	Gage 6, Line 4	+0.4			
	Gage 8, Line 2	+0.4	+0.4	0.0	+9.55
	Gage 5, Line 4	+0.4			

Table 2 Check on Unit Strain Values and Stress Calculation (Unsymmetrical Loading)

Longitudinal stresses at midspan (psi)							
Source	0	1	2	3	4	5	6
Ridge							
Beam method	+152.5	+78.2	-45.9	-89.4	-45.9	+78.2	+152.5
Winter and Pei's method	+143.1	-286.0	+744.0	-1178.0	+744.0	-286.0	+143.1
Gesund's method	-247.8	+231.9	+6.4	-236.5	+6.4	+231.9	-247.8
Slope deflection method	-248.9	+235.4	+6.8	-241.2	+6.8	+235.4	-248.9
ASCE recommended method	-249.7	+236.4	+5.8	-238.0	+5.8	+236.4	-249.7
Energy method	-242.2	+240.0	+5.0	-245.0	+5.0	+240.0	-242.2
Longitudinal stresses at 2" from end (psi)							
Beam method	+42.8	+21.9	-12.9	-25.2	-12.9	+21.9	+42.8
Winter and Pei's method	+34.7	-69.4	+208.4	-294.0	+208.4	-69.4	+34.7
Gesund's method	-51.4	+40.5	+35.7	-109.0	+35.7	+40.5	-51.4
Slope deflection method	-50.3	+42.6	+33.3	-110.2	+33.3	+42.6	-50.3
ASCE recommended method	-52.4	+41.6	+35.8	-108.9	+35.8	+41.6	-52.4
Energy method	-51.3	+44.7	+35.0	-109.4	+35.0	+44.7	-51.3



* + indicates tension, - indicates compression

Table 3 : Theoretical Stresses at Ridges (symmetrical loading)

Longitudinal stresses at midspan, (psi)							
Ridge	0	1	2	3	4	5	6
Source							
Winter and Pel's method	-523.0*	+1045.1	-1190.2	+704.3	-173.7	+63.5	-31.4
Gesund's method	+356.1	+189.5	-281.9	-62.9	+151.4	-16.3	-82.7
Slope deflection method	+353.1	+184.4	-275.4	-67.2	+163.1	-16.8	-86.8
ASCE recommended method	+356.1	+180.8	-275.1	-66.2	+162.0	-15.7	-84.3
Energy method	+362.8	+189.2	-284.8	-52.0	+155.2	-16.8	-91.2
Longitudinal stresses at 2" from end (psi)							
Winter and Pel's method	-127.1	+254.3	-289.4	+170.6	-42.2	+15.3	-7.6
Gesund's method	+61.8	+86.0	-119.0	+17.0	+26.4	-0.97	-20.9
Slope deflection method	+60.8	+89.6	-119.3	+17.0	+28.4	-1.9	-18.7
ASCE recommended method	+59.6	+90.9	-119.2	+15.3	+29.4	-0.4	-23.8
Energy method	+63.1	+87.1	-123.4	+13.0	+26.8	-1.1	-24.9

* + indicates tension, - indicates compression.

Table 4: Theoretical Stresses at Ridges (unsymmetrical loading)



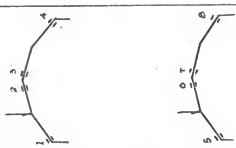
Gage point		1	2	3	4	5	6	7	8
Source									
Beam method		+54.6* (-77.4)	-80.5 (+67.0)	-80.5 (+67.0)	+54.6 (-77.4)	+15.3 (-68.6)	-23.4 (-60.0)	-23.4 (-60.0)	+15.3 (-68.6)
Winter and Pel's method		-175.1 (-172.2)	-696.2 (+184.1)	-696.2 (+184.1)	-175.1 (-172.2)	-49.2 (-201.1)	-195.5 (+235.0)	-195.5 (+235.0)	-49.2 (-201.1)
Gesund's method		+206.4 (-14.3)	-187.6 (-23.5)	-187.6 (-23.5)	+206.4 (-14.3)	+39.9 (-18.4)	-80.2 (+37.3)	-80.2 (+37.3)	+39.9 (-18.4)
Slope deflection method		+208.8 (-13.3)	-191.7 (-21.8)	-191.7 (-21.8)	+208.8 (-13.3)	+41.6 (-14.9)	-81.6 (+39.4)	-81.6 (+39.4)	+41.6 (-14.9)
ASCE recommended method		+211.8 (-12.2)	-188.2 (-23.1)	-188.2 (-23.1)	+211.8 (-12.2)	+40.9 (-16.3)	-79.3 (+35.5)	-79.3 (+35.5)	+40.9 (-16.3)
Energy method		+215.0 (-10.8)	-195.0 (-20.4)	-195.0 (-20.4)	+215.0 (-10.8)	+42.8 (-12.5)	-80.2 (+37.3)	-80.2 (+37.3)	+42.8 (-12.5)
Experimental values		+241.0	-245.0	-245.0	+241.0	+48.9	-58.4	-58.4	+48.9



* Stresses at each gage point in psi, + indicates tension, - indicates compression.
 ** Values in parentheses are percent differences.

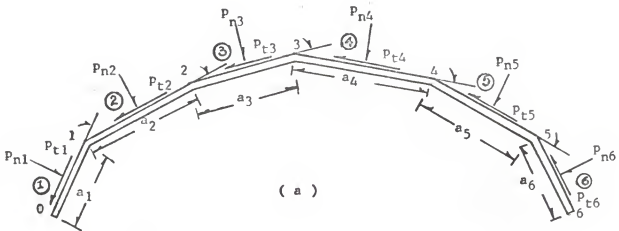
Table 5: Comparison of Theoretical and Experimental Stresses for Symmetrical Loading

Gage point Source	1	2	3	4	5	6	7	8
Winter and Pei's method	+807.1* (+543.6)	+372.8 (-432.1)	+529.3 (-331.2)	+38.3 (+25.3)	+196.3 (+221.0)	+78.9 (-204.0)	+128.6 (+1090)	+9.2 (-3.1)
Gesund's method	+139.2 (+11.2)	-106.7 (-4.7)	-20.1 (+22.5)	+1.6 (-94.5)	+64.2 (+5.1)	-10.8 (-62.8)	+18.9 (+76.5)	+1.9 (-80.0)
Slope deflection method	+135.4 (+8.2)	-108.8 (-2.9)	-21.0 (+28.1)	+2.4 (-92.2)	+68.4 (+11.8)	-10.2 (-63.4)	+19.28 (+79.5)	+1.3 (-86.5)
ASCE recommended method	+132.3 (+5.7)	-108.0 (-3.7)	-20.8 (+26.7)	+3.2 (-89.5)	+68.5 (+11.9)	-11.5 (-62.2)	+18.1 (+69.0)	+2.8 (-70.5)
Energy method	+138.6 (+10.7)	-98.6 (-12.0)	-20.2 (-27.8)	+1.6 (-94.5)	+66.4 (+8.5)	-12.5 (-55.1)	+16.8 (+56.8)	+2.1 (-77.5)
Experimental values	+125.1	-112.1	-16.4	+30.4	+61.2	-27.8	+10.7	+9.5

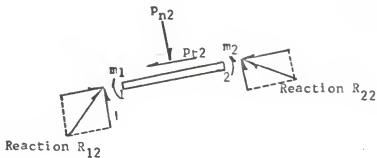


* Stresses at each gage point in psi, + indicates tension, - indicates compression.
 ** Values in parentheses are percent differences.

Table 6 : Comparison of Theoretical and Experimental Stresses
 for Unsymmetrical Loading.



Note: p_n is normally a distributed load and is indicated by a single arrow only for convenience.



All forces, loads, reactions, moments, and angles are regarded as positive as shown in (a) and (b).

Fig.1 Sign and Loading Convention for Gesund's Method

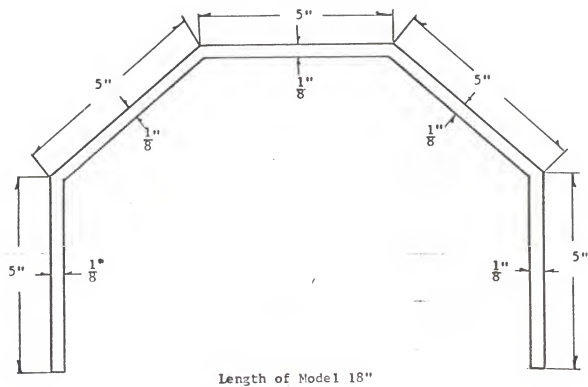
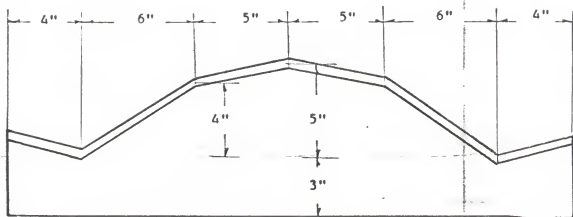


Fig.2 Model Used in References 17 and 18



Length of model 70"

Basic dimension of Model A and Model B

Fig. 3 Model Used in Reference 19

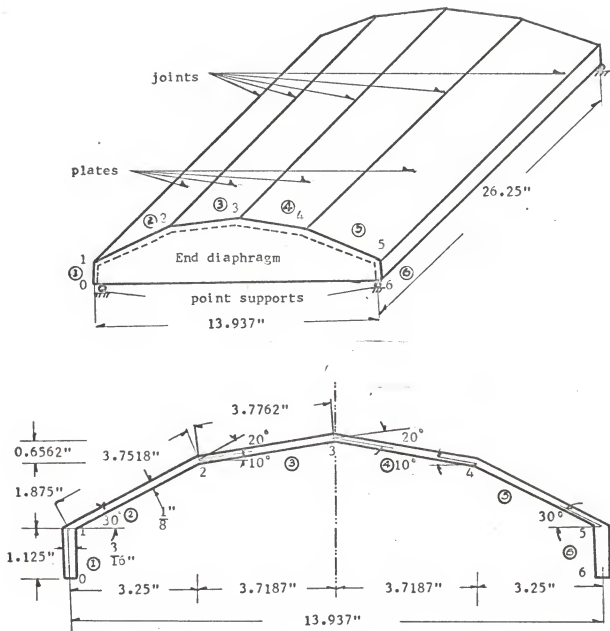


Fig. 4 Simple Span Folded Plate Model

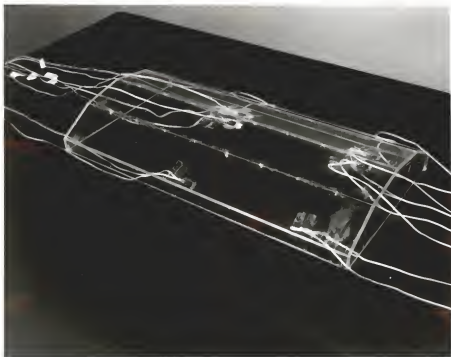
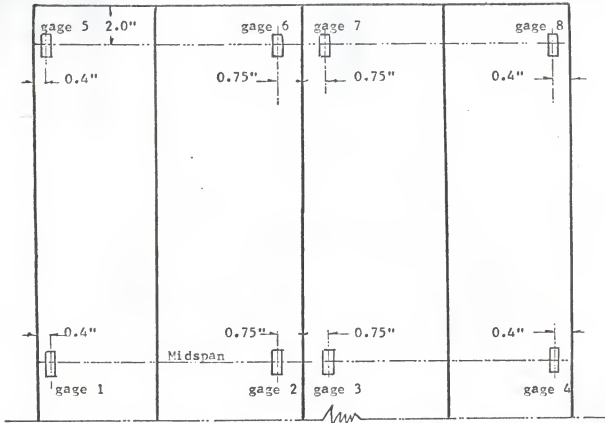
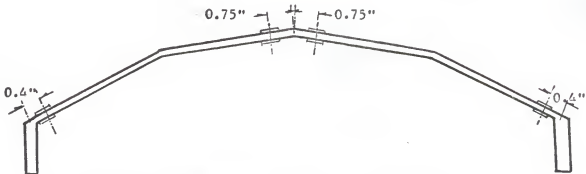


Fig. 5 Folded Plate Model



(a) Layout of location of strain gages on plan view



(b) Location of strain gages on cross section

Fig. 6 Location of Strain Gages

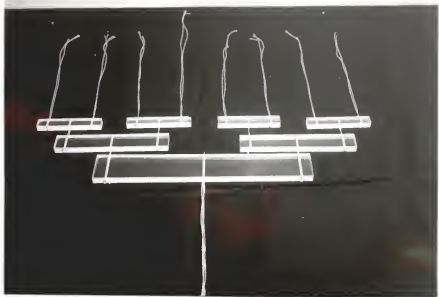


Fig. 7 Loading Tree System

(a) 1/8" coupon

(b) 3/16" coupon

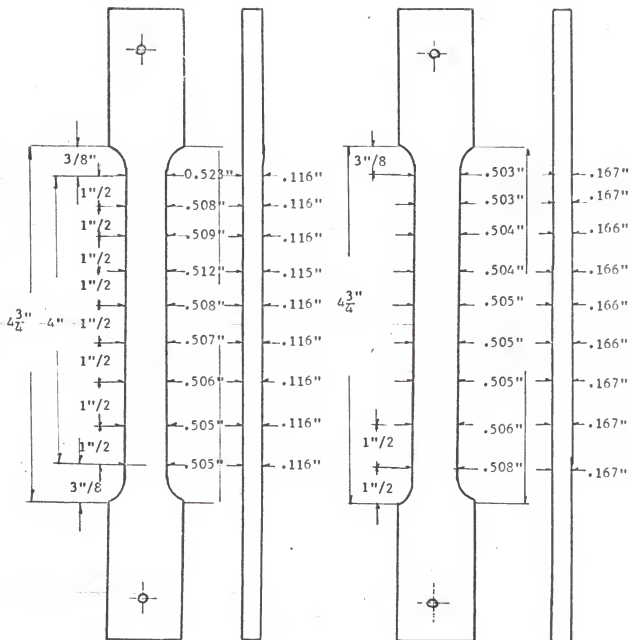


Fig. 8 Tensile Coupon Specimens

Tensile Coupon Test
coupon section: 1/8" x 1/2"
constant loading: 20 lb
total stress: 320 psi
date: July 5, 1968

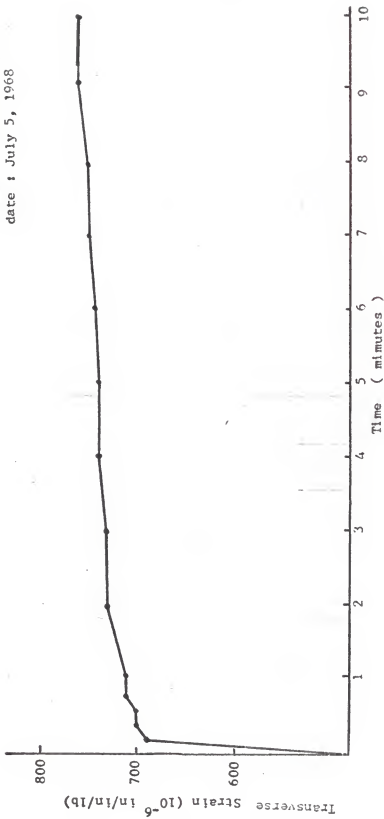


Fig. 9 Relationship between Transverse Strain and Time

Longitudinal Gage Reading
(Readings taken in 5 minute intervals)
coupon section: 1/8" x 1/2"
date: July 11, 1968

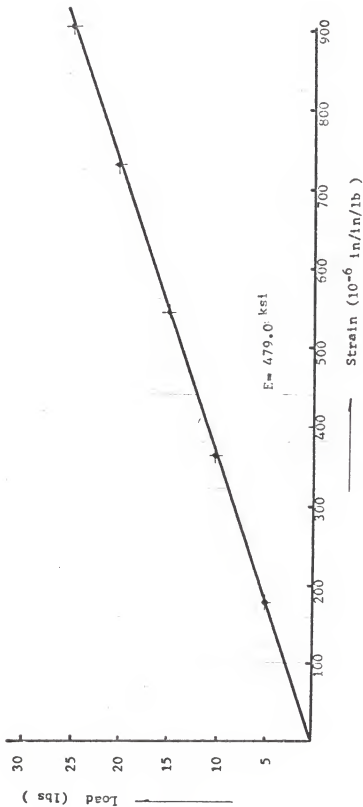


Fig. 10 Load-Strain Relationship for Tensile Coupon

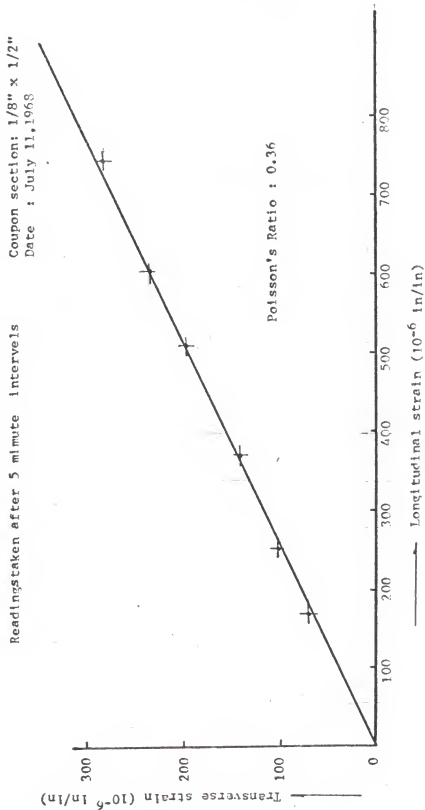


Fig. 11 Relationship between Transverse and Longitudinal Strains

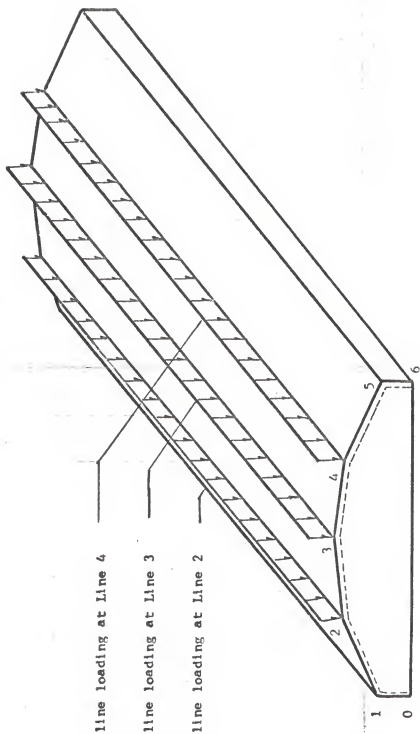
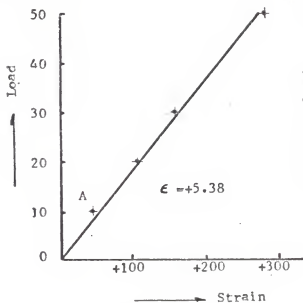
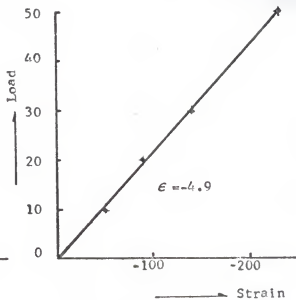


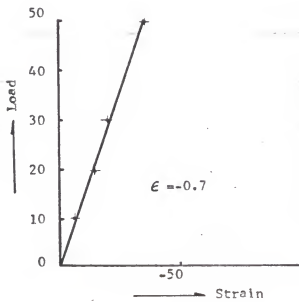
Fig. 12 Location of Line Loadings



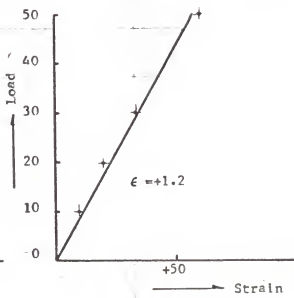
Gage point 1



Gage point 2



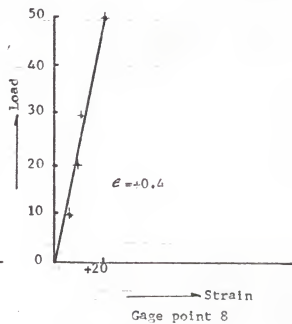
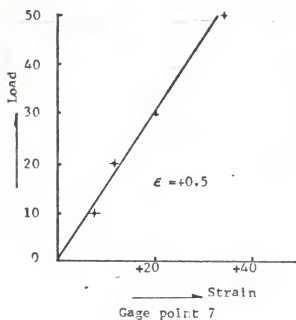
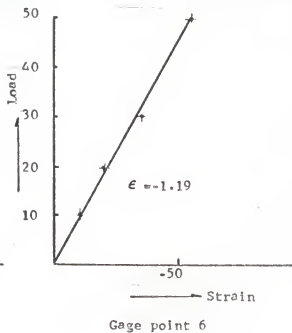
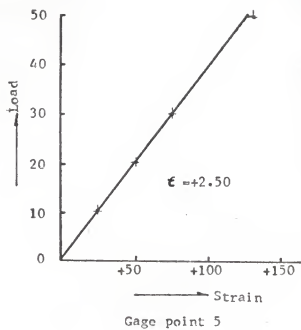
Gage point 3



Gage point 4

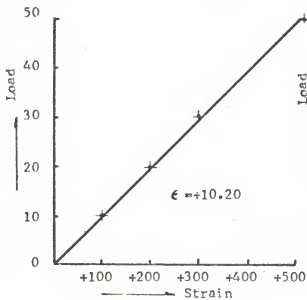
Load : lb
 Strain : 10^{-6} in/in
 ϵ : 10^{-9} in/in/lb

Fig.13 Line loading on Line 2

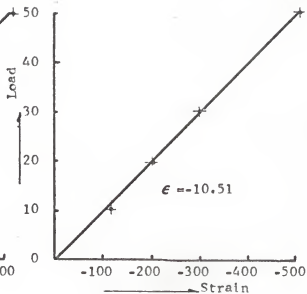


Load ; lb
 Strain: 10^{-6} in/in
 ϵ : 10^{-6} in/in/lb

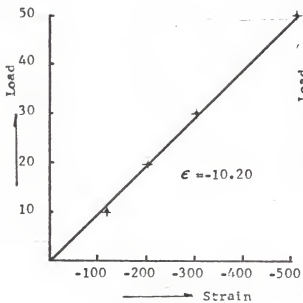
Fig. 14 Line loading on line 2



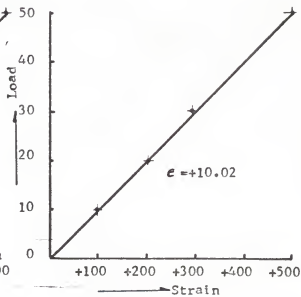
Gage point 1



Gage point 2



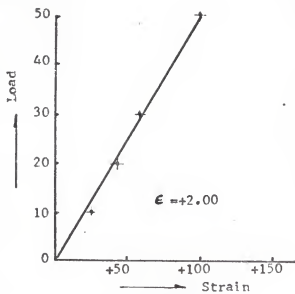
Gage point 3



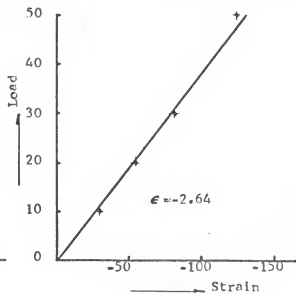
Gage point 4

Load : 1b
 Strain: 10^{-6} in/in
 ϵ : 10^{-6} in/in/lb

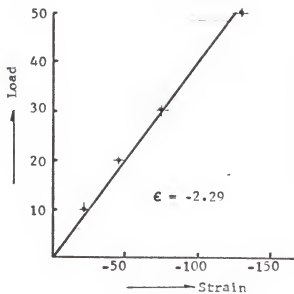
Fig.15 Line loading on Line 3



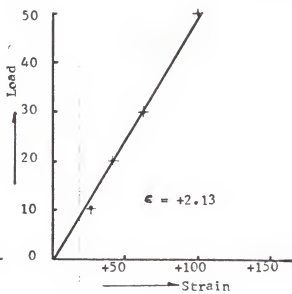
Gage point 5



Gage point 6



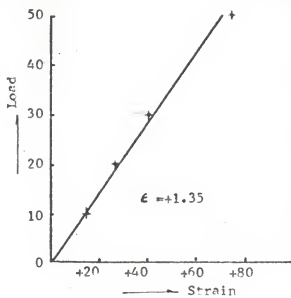
Gage point 7



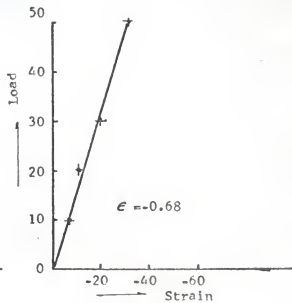
Gage point 8

Load : lb
 Strain : 10^{-6} in/in
 ϵ : 10^{-6} in/in/lb

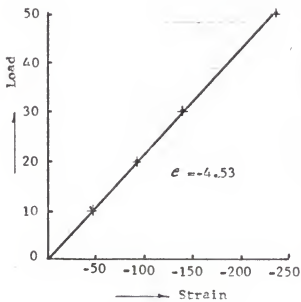
Fig.16 Line loading on Line 3



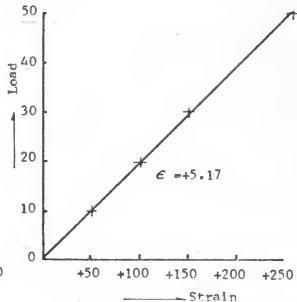
Gage point 1



Gage point 2



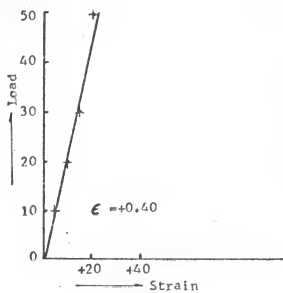
Gage point 3



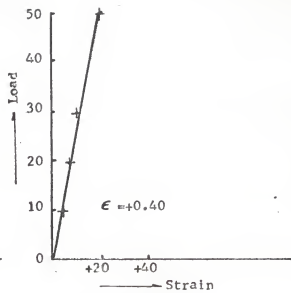
Gage point 4

Load : lb
 Strain: 10^{-6} in/in
 ϵ : 10^{-6} in/in/lb

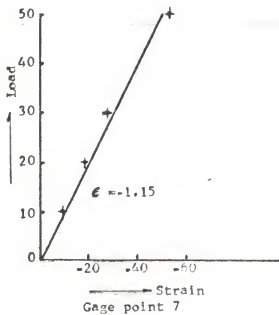
Fig. 17 Line loading on Line 4



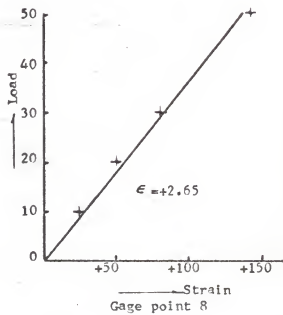
Gage point 5



Gage point 6



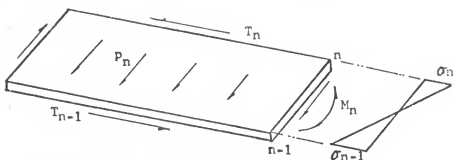
Gage point 7



Gage point 8

Load : lb
 Strain : 10^{-6} in/in
 ϵ : 10^{-6} in/in/lb

Fig. 18 Line loading on Line 4



(a) Longitudinal Bending Stresses

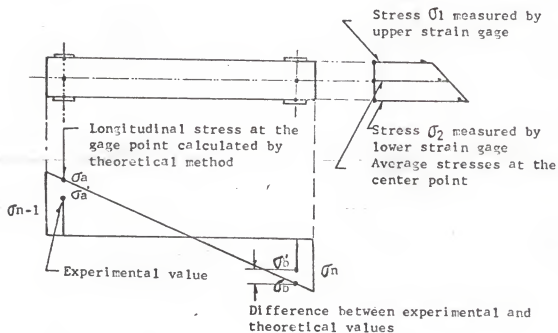
(b) Difference between longitudinal stresses:
theoretical vs experimental values

Fig. 19 Comparison of Longitudinal Plate Bending Stresses

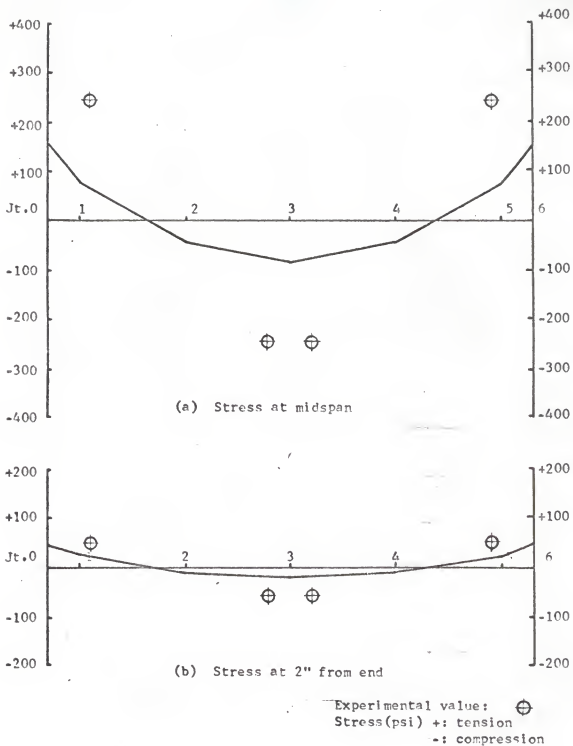
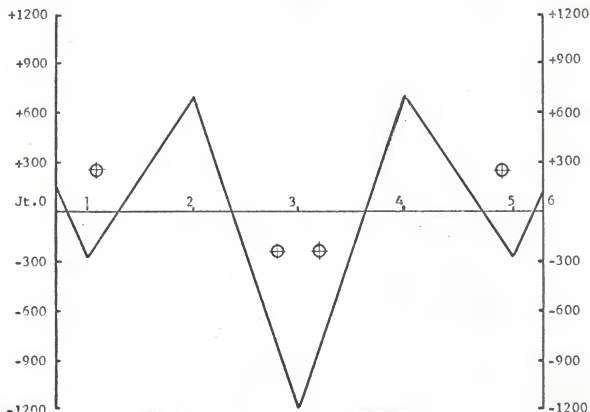
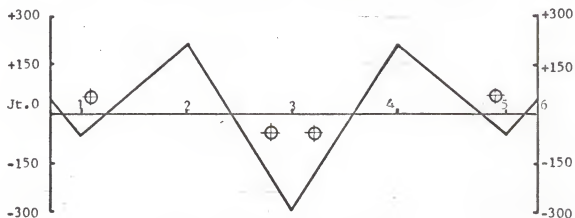


Fig. 20 Comparison of Experimental Results with Beam Method (symmetrical loading)



(a) Stress at midspan



(b) Stress at 2" from end

Experimental value: \oplus
 Stress(psi) +:tension
 -:compression

Fig. 21 Comparison of Experimental Results with Winter and Pei's Method(symmetrical loading)

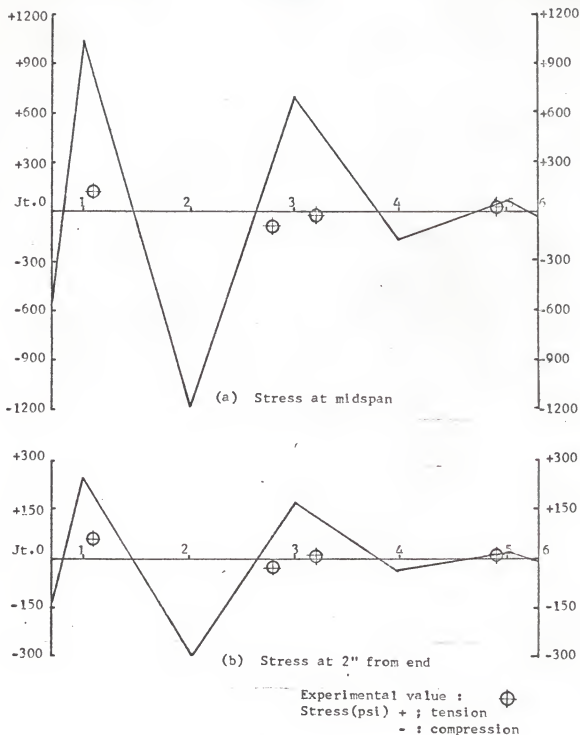


Fig. 22 Comparison of Experimental Results with Winter and Pei's Method (unsymmetrical loading)

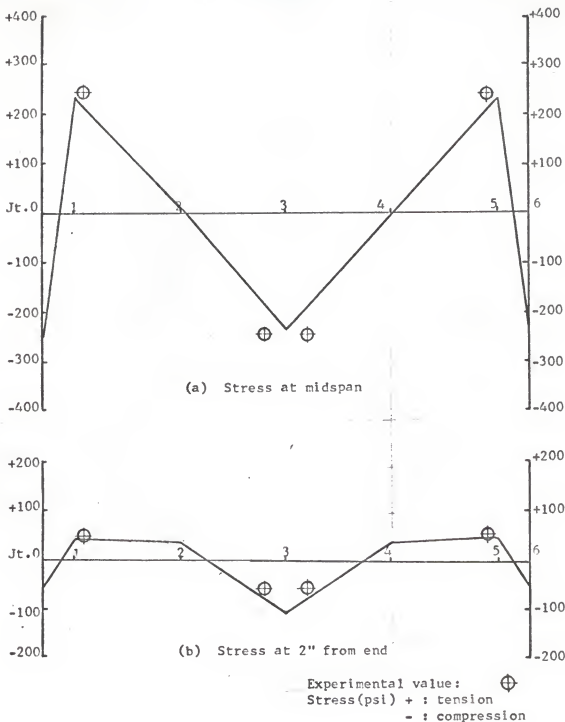


Fig. 23 Comparison of Experimental Results with Gesund's Method (symmetrical loading)

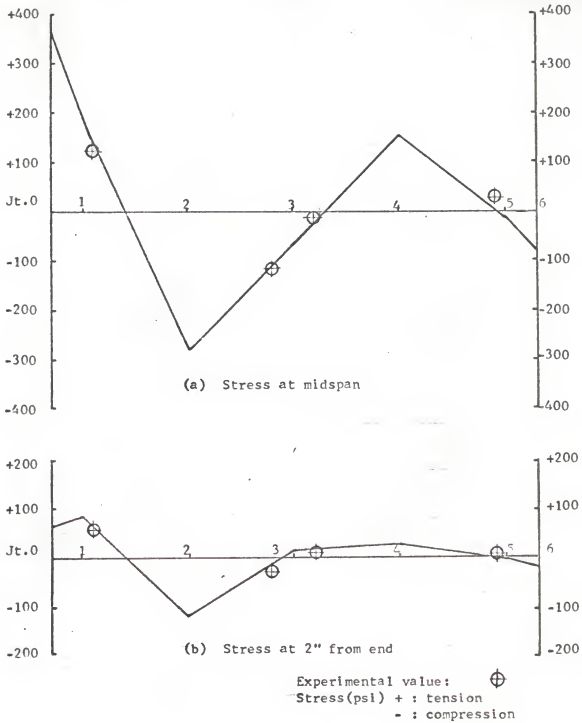
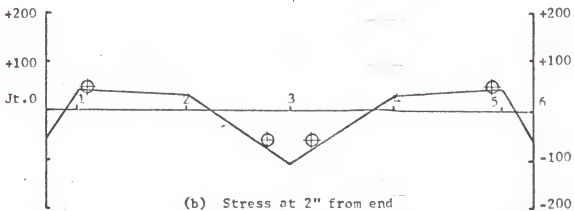
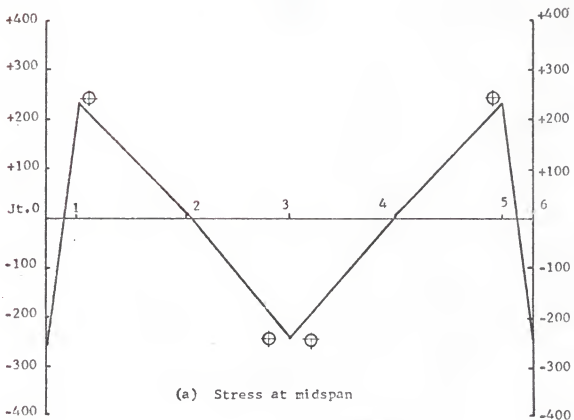


Fig. 24 Comparison of Experimental Results with Gesund's Method(unsymmetrical loading)



Experimental value: \oplus
 Stress(psi) + : tension
 - : compression

Fig. 25 Comparison of Experimental Results with Slope Deflection Method(symmetrical loading)

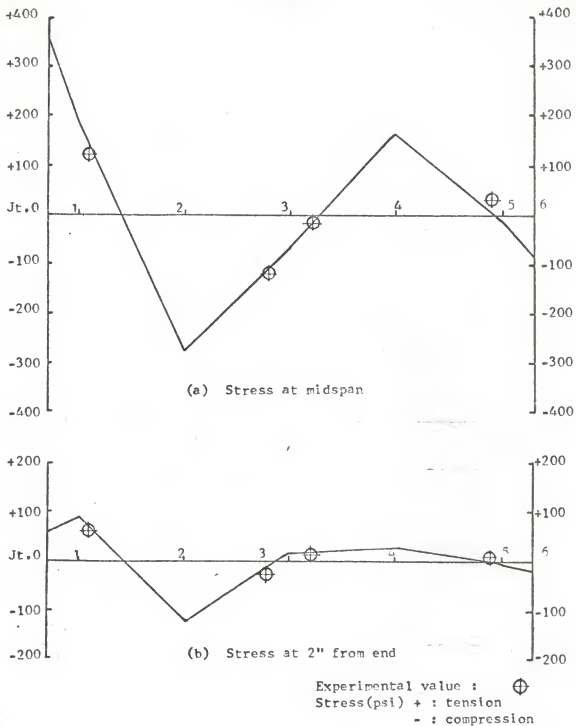


Fig. 26 Comparison of Experimental Results with Slope Deflection Method (unsymmetrical loading)

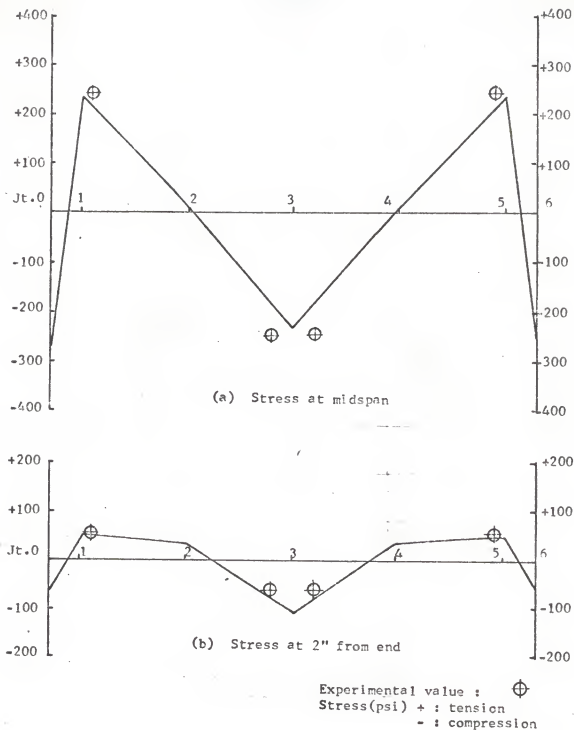


Fig. 27 Comparison of Experimental Results with ASCE Recommended Method (symmetrical loading)

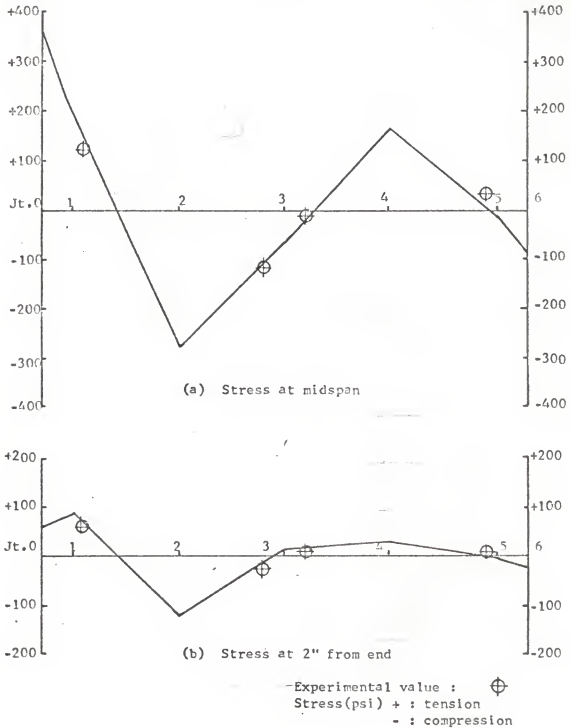


Fig. 28 Comparison of Experimental results with ASCE Recommended Method (unsymmetrical loading)

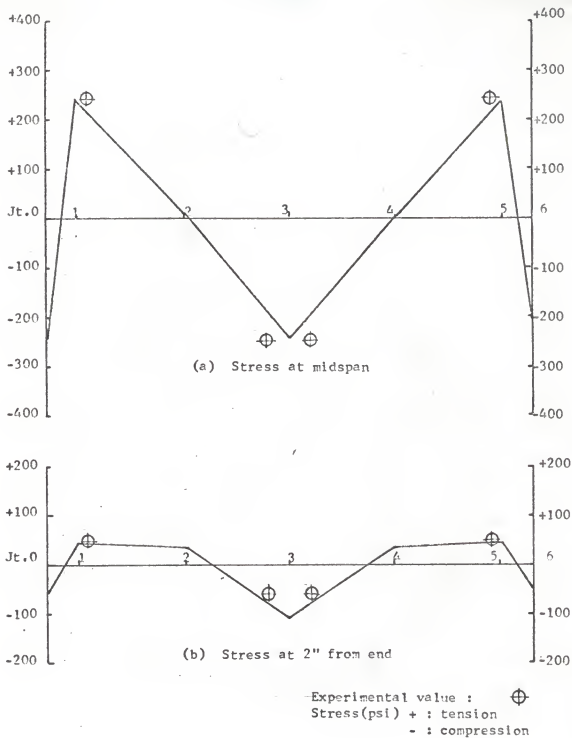


Fig. 29 Comparison of Experimental Results with Energy Method (symmetrical loading)

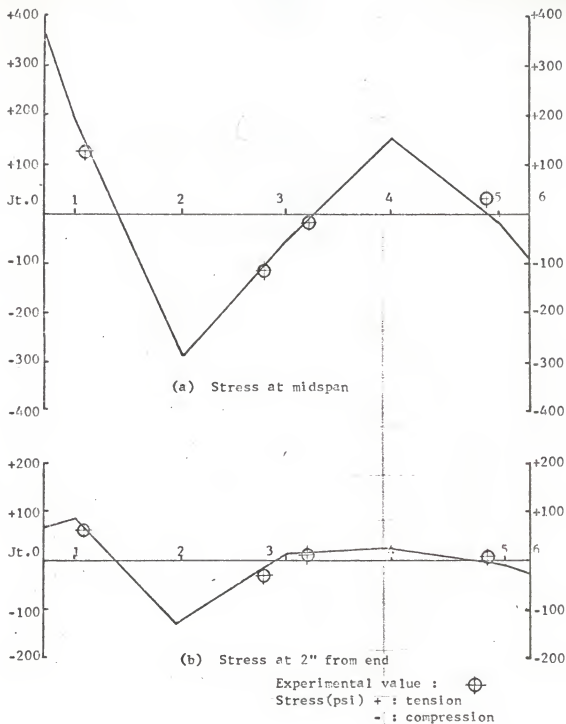


Fig. 30 Comparison of Experimental Results with Energy Method (unsymmetrical loading)

A MODEL STUDY OF A FOLDED PLATE STRUCTURE

by

SHIH YING CHANG

Diploma, Taipei Institute of Technology, Taiwan, China

AN ABSTRACT OF A MASTER'S THESIS

submitted in partial fulfillment of the

requirements for the degree

MASTER OF SCIENCE

Department of Civil Engineering

Kansas State University

Manhattan, Kansas

1969

ABSTRACT

A study of a simple span, plexiglas, folded plate model consisting of six plates is presented. The purpose of the study was twofold:

- (1) To verify theories used in the present day analysis of folded plate systems by means of a structural model; and
- (2) To investigate testing techniques for three-dimensional structural models fabricated from plexiglas.

Preliminary tests conducted to determine the creep characteristics, Poisson's ratio and the Modulus of Elasticity of the plexiglas, and also to verify the behavior of strain gages are described in detail. The various experimental setups are also described and illustrated.

Analytical values of longitudinal, plate bending stresses obtained using the beam method, Winter and Pei's method, Gesund's method, the slope deflection method, the ASCE recommended method, and the energy method are compared with experimental results.

It is concluded that the analysis methods which neglect relative joint displacements yield stress values which are significantly in error with respect to magnitude and distribution across the cross section, while methods which consider relative joint displacements, although the analytic procedures are quite different, yield results which are practically equivalent and which result in good agreement with the experimental values.

It is also concluded that, when proper precautions are taken, plexiglas can be used as a model material with consistent results and the model tests can be performed very simply.